Gold Nanoparticle Uptake in Tumor Cells: Quantification and Size Distribution by sp-ICPMS

Johanna Noireaux, Romain Grall, Marie Hullo, Sylvie Chevillard, Caroline Oster, Emilie Brun, Cécile Sicard-Roselli, Katrin Loeschner, Paola Fisicaro

separations

MDPI

Article

Gold Nanoparticle Uptake in Tumor Cells: Quantification and Size Distribution by sp-ICPMS

Johanna Noireaux [1], Romain Grall [2], Marie Hullo [2], Sylvie Chevillard [2], Caroline Oster [1], Emilie Brun [3], Cécile Sicard-Roselli [3], Katrin Loeschner [4] and Paola Fisicaro [1,*]

1 Department for biomedical and inorganic chemistry, LNE, 75015 Paris, France; johanna.noireaux@lne.fr (J.N.); caroline.oster@lne.fr (C.O.)
2 Experimental cancerology laboratory, CEA, 92260 Fontenay-aux-Roses, France; romain.grall@cea.fr (R.G.); marie.hullo@cea.fr (M.H.); sylvie.chevillard@cea.fr (S.C.)
3 Laboratoire de Chimie Physique, UMR CNRS 8000, Université Paris Sud, 91405 Orsay, France; emilie.brun@u-psud.fr (E.B.); cecile.sicard@u-psud.fr (C.S.-R.)
4 National Food Institute, Technical University of Denmark, 2800 Kgs. Lyngby, Denmark; kals@food.dtu.dk
* Correspondence: paola.fisicaro@lne.fr

Received: 31 October 2018; Accepted: 13 December 2018; Published: 9 January 2019

Abstract: Gold nanoparticles (AuNPs) are increasingly studied for cancer treatment purposes, as they can potentially improve both control and efficiency of the treatment. Intensive research is conducted in vitro on rodent and human cell lines to objectify the gain of combining AuNPs with cancer treatment and to understand their mechanisms of action. However, using nanoparticles in such studies requires thorough knowledge of their cellular uptake. In this study, we optimized single particle ICPMS (sp-ICPMS) analysis to qualify and quantify intracellular AuNP content after exposure of in vitro human breast cancer cell lines. To this aim, cells were treated with an alkaline digestion method with 5% TMAH, allowing the detection of gold with a yield of 97% on average. Results showed that under our experimental conditions, the AuNP size distribution appeared to be unchanged after internalization and that the uptake of particles depended on the cell line and on the exposure duration. Finally, the comparison of the particle numbers per cell with the estimates based on the gold masses showed excellent agreement, confirming the validity of the sp-ICPMS particle measurements in such complex samples.

Keywords: sp-ICPMS; gold nanoparticles; tumor cells; nanoparticle uptake

1. Introduction

In 2016, 51 FDA-approved nanomedicines were available and 77 nanoproducts were on clinical trials, among which a large number were related to oncology [1]. Nanoparticles are thus increasingly developed for cancer diagnosis and therapy, mainly as drug nanocarriers, but other applications are currently being investigated: in particular, gold nanoparticles (AuNPs) are studied as promising contrast agents and as radiosensitizers in X-ray therapy (also known as high Z radioenhancement) [2]. Two major barriers to break down in nanomedicine are the uptake of nanoparticles by normal tissues and the nanoparticles' inability to efficiently penetrate solid tumors. Overcoming these hurdles is of great interest during the development of efficient gold nanoparticles for therapy, since mass and number of internalized AuNPs and their aggregation state could be overriding parameters for cellular responses. Different pathways of internalization could drive to huge variation in intracellular accumulation of AuNPs and lead to different aggregation states or to sequestration in cellular compartments, and thus to different biological activities. Studying these issues requires robust methods to characterize and quantify gold nanoparticle uptake into cells.

To this aim, single particle ICPMS (sp-ICPMS) appears to be a powerful tool in enabling the analysis of particle sizes, particle mass concentrations, and particle number concentrations. This method is based on ICPMS instruments that allow targeting of inorganic nanoparticles even in a complex matrix by using fast scanning to analyze one particle individually in diluted samples. It has been so far successfully applied to a variety of samples from the environment [3,4], food products [5,6], manufactured goods [7–9], or from biological origins [10–14]. Performing an analysis of biological samples by sp-ICPMS requires a digestion step to release the particles from their biological matrix. At least two methods are currently in use, either an alkaline or an enzymatic digestion. Plant digestions with Macerozyme R-10 (multicomponent enzyme mixture) resulted in a high recovery rate for many different nanoparticles, such as gold nanoparticles [11], but also platinum [12], palladium [15], and cerium oxide nanoparticles [16]. In animal or human tissues, the protease Proteinase K is used. Enzymatic digestion with Proteinase K at an enzyme concentration of around 4 µg Proteinase K per mg wet tissue resulted in a satisfactory size distribution but a 60% lower recovery rate of gold nanoparticles from rat spleen in comparison to alkaline digestion with tetramethyl ammonium hydroxide (TMAH) [17]. In contrast, silver nanoparticles were satisfactorily recovered from human placenta tissue at an enzyme concentration of 60 µg Proteinase K per mg wet tissue [18] and from chicken meat at an enzyme concentration of 4 µg Proteinase K per mg wet tissue [19]. Another study was able to make successful use of alkaline digestion for both gold and silver nanoparticle extraction from ground beef, *Daphnia magna*, and *Lumbriculus variegatus* [20]. These studies clearly show that nanoparticle extraction must currently be optimized and verified for each nanoparticle–sample pair, as no versatile procedure is available yet. In this study, we optimized the sp-ICPMS method for the analysis of 32 nm PEGylated gold nanoparticles internalized after in vitro exposure of human breast cancer cell lines. PEGylation is among the most common functionalizations, as it lowers opsonization and thus the capture of the nanoparticles by the immune system [21]. Our aim was to validate the use of sp-ICPMS in analyzing intracellular particle size distribution and to quantify their average mass and number per cell for biological and medical research dealing with AuNPs. First, an alkaline digestion procedure was adapted to our samples, then the results obtained with sp-ICPMS were compared to ICPMS acid digestion for validation, and finally the particle numbers per cell were estimated through three different calculation methods.

2. Materials and Methods

2.1. Instruments

Both ICPMS and sp-ICPMS measurements were performed on a Thermo iCAPQ quadrupole ICPMS (Thermo Fischer Scientific, Bremen, Germany) fitted with a 400 µL/min Micromist concentric quartz nebulizer (Glass Expansion, Melbourne, Australia) and a Peltier cooled cyclonic spray chamber (Thermo Fischer Scientific, Bremen, Germany). The instrument daily performance was checked with a tune solution containing Ba, Bi, Ce, Co, In, Li, and U at 1.0 ng/g concentration in 2% HNO_3 and 0.5% HCl. Measurements by sp-ICPMS were performed in time-resolved analysis, and signals (in cps) were exported. Calculations were performed with a custom-made Excel spreadsheet based on the tool developed by Peters and colleagues [22], modified to include transport efficiency calculations using the size method [23]. The sample uptake was determined gravimetrically by weighing ultrapure water three times for 5 min. Operating parameters of the Thermo iCAPQ instrument are listed in Table 1.

2.2. Reagents

Ultrapure water (18.2 mΩ/cm) was obtained from Merck Millipore (Guyancourt, France). Mono-elemental gold solutions and TMAH 25% *w*/*w* were obtained from Alfa Aesar (Karlsruhe, Germany), and bovine serum albumin (BSA) 30% in 0.85% sodium chloride was obtained from Sigma Aldrich (Saint-Louis, MO, USA). High-purity (Suprapur) hydrochloric and nitric acids were purchased from Merck (Darmstadt, Germany). Two gold nanoparticle suspensions were used as

reference materials for transport efficiency: NIST RM8012 and BBI 60 nm, obtained from British Biocell International (Crumlin, UK). For calculations, we used the average value of all sizes reference value for 30 nm NIST RM8012 (26.80 ± 0.38 nm, $k = 2$), and we used the product datasheet value of 61.5 ± 4.9 nm for BBI 60 nm.

Table 1. Operating parameters of Thermo iCAPQ in ICPMS and single particle (sp)-ICPMS mode.

	ICP-MS	**sp-ICPMS**
Plasma power (W)	1550	1550
Plasma gas (mL/min)	0.8	0.8
Cool gas (mL/min)	14	14
Nebulizer gas (mL/min)	1.0	1.0
Spray chamber	Quartz cyclonic spray chamber	
Nebulizer	Quartz concentric	
Measurement mode	STD	STD
Isotope	197 Au	197 Au
Sample uptake rate (g/min)	~0.4	0.259 ± 0.008
Dwell time (ms)	200	5
Number of scans per measurement	60	18000

2.3. Samples and Sample Preparation

2.3.1. Gold Nanoparticle Synthesis and Functionalization

Gold nanoparticles were prepared through the Turkevich procedure [24] by mixing trisodium citrate (4.6 mL, 1% (w/v)) with aqueous $KAuCl_4$ solution (0.1 mmol, 100 mL), as previously published [25]. Raw batches were functionalized with thiolated polyethylene glycol (PEG) with a molecular weight of 1000 and an amine moiety (SH-PEG1000-NH_2, Interchim, Montluçon, France), and 25 mL of a 40 µM PEG aqueous solution were added to 90 mL of a gold AuNP solution (approximately 1 nM, 11,000 PEG/AuNP) and mixed vigorously at 4 °C during 30 min. The suspension was left undisturbed overnight. Cold temperature was used to promote S anchoring as mentioned in Xia et al. [26]. Three cycles of centrifugation at 18,000 g for 8 min were then performed to remove the excess reactants. The nanoparticles were characterized by UV-visible spectroscopy to estimate their concentration, transmission electron microscopy (TEM) to measure the diameter of their gold core, and dynamic light scattering (DLS) and zetametry to confirm their functionalization. For TEM experiments, 2 µL of AuNP stock solution was deposited onto a formvar/carbon-coated copper grid for 3 min and imaged with a JEOL 1400 TEM instrument (JEOL USA, Peabody, MA, USA) operating at 80 kV. AuNP size was determined from recorded images with ImageJ 1.41 software. For DLS, AuNPs were analyzed on a Malvern NanoZS3600 (Malvern Panalytical, Almelo, Netherlands) at 25 °C (633 nm laser, backscatter mode) after dilution in water (0.08 nM). The hydrodynamic diameter was extracted from intensity measurements, ignoring the rotational diffusion of particles. Zeta potentials were measured on a Malvern instrument NanoZS3600 in 1 mL folded capillary cells on 1 nM AuNP samples in water with a fixed voltage at 150 mV at 25 °C.

According to TEM, AuNPs had a typical quasi-spherical, slightly ovoid shape from Turkevich synthesis and a mean of 31.9 ± 5.3 nm in diameter (Figure 1). Functionalization was assessed by the 5 nm redshift of the plasmon band, the increase of the hydrodynamic diameter from 40.6 ± 1.0 nm for nonfunctionalized, nonwashed nanoparticles to 66.0 ± 2.2 nm for thiolated nanoparticles, and the sign inversion of the zeta potential in ultrapure water from −39 ± 2 mV for citrate-capped AuNPs to 30 ± 5 mV for AuNP @S-PEG1000-NH_3^+.

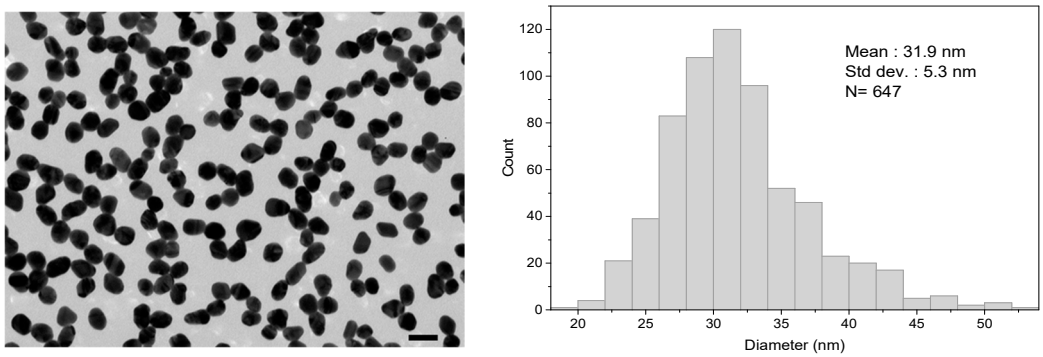

(**a**) (**b**)

Figure 1. (**a**) Representative TEM images and (**b**) size distribution histogram of the PEGylated gold nanoparticles (AuNPs) used in the present study: 647 nanoparticles were manually measured to obtain this distribution. Scale bar in the right bottom corner of (a): 50 nm.

2.3.2. Cell Growth

Tumor cell lines MDAMB231 (ATCC number HTB-26) and T47D (ATCC number HTB-133) were routinely grown at 37 °C in a humidified atmosphere of 5% CO_2 and 95% air, in Dulbecco's modified Eagle medium (DMEM), GlutaMAX supplemented with 10% (v/v) heat-inactivated fetal bovine serum (Sigma-Aldrich, Saint-Louis, MO, USA) and 1 mM antibiotic-antimycotic (Invitrogen, Carlsbad, CA, USA. Briefly, cells were seeded in 25 cm^2 flasks, 500,000 cells and 1,000,000 cells per flask for MDAMB231 and T47D, respectively. Twenty-four hours later, the medium was removed and fresh medium of AuNP suspension was added, depending on the sample, following the plan detailed in Table 2. After 6 h and 24 h of exposure, supernatants were removed and cells were washed twice with PBS buffer containing calcium and magnesium (Invitrogen), before being harvested with trypsin (Invitrogen). Trypsin was inactivated with fresh complete medium, before centrifugation (1200 rpm, 5 min). Pellets were resuspended in fresh complete medium, and then cells were counted twice (Trypan Blue) and centrifuged again. Finally, to preserve the sample stability, pellets were prepared for sp-ICPMS less than 12 h after centrifugation.

Table 2. Number of cells per condition and gold mass in the medium at the beginning of exposure.

Sample	Gold Mass in Cell Medium	Number of Cells
MDAMB231 (control)	0 µg	2.21×10^6
MDAMB231 (6 h)	250 µg	2.01×10^6
MDAMB231 (24 h)	250 µg	2.25×10^6
T47D (control)	0 µg	1.8×10^6
T47D (6 h)	250 µg	2.49×10^6
T47D (24 h)	250 µg	2.21×10^6

2.3.3. Sample Preparation for Total Gold Mass Concentration Measurements

For total gold mass concentration measurements, samples were digested in 2 mL aqua regia in quartz vials, then microwaved in a Discover SP instrument (CEM, Saclay, France) for 15 min with a 5 min temperature increase to reach a 200 °C plateau, which was maintained for 10 min. After digestion, the samples were diluted in ultrapure water for ICPMS introduction. All dilutions were performed gravimetrically. Blanks were carefully checked, and at least one aqua regia blank per day was digested and diluted following the same procedure as the samples. Digestion blanks did not show any additional gold compared to diluted aqua regia.

To obtain gold recovery rates, one cell test sample (T47D test) was split in two aliquots: the first one was measured by ICPMS after acid digestion, whereas the other one was measured by sp-ICPMS

after alkaline digestion. For the other cell samples, acid digestion was performed on 500 µL of the suspensions obtained after the alkaline digestion of a whole sample.

2.3.4. Sample Preparation for Sp-ICPMS Measurement and Method Validation

Samples were digested for sp-ICPMS measurements using an alkaline method with TMAH based on two previously published methods for biological tissues [17,20]. The TMAH concentration and the addition of BSA were optimized for the specific samples of the present study. The best results were obtained when the samples were digested overnight in 1 mL of 5% TMAH with 10 µL of BSA 1.5 mg/mL. After this digestion step, the suspensions were diluted to the desired concentration in 1% TMAH. Measurements of 1% TMAH were regularly performed for blank corrections, and the instrument was rinsed in ultrapure water for 4 min between each measurement. Control cell samples that were not exposed to gold did not show any additional signal compared to blanks.

All ICPMS measurements on cell samples were performed in a single day following overnight digestion to avoid compromising the samples' stability. Whenever possible, at least two different dilutions of samples were performed, and the average results and standard deviation were reported.

For method validation, AuNP mass concentrations measured by sp-ICPMS were compared to the ICPMS mass concentrations obtained after classic acid digestion and the diameters obtained on reference gold nanoparticles were compared to their reference diameters.

2.4. Calculations

2.4.1. Limits of Detection and Uncertainty

The limit of detection (LOD) by ICPMS was determined as the smallest measurement of dissolved gold standard corrected from the dilutions performed for sample preparation. For sp-ICPMS, the LOD for particle mass concentration was calculated using the ISO 19590 standard equation [27].

In practice, the gold dissolved standards ranged from 0.02 ng/g to 1 ng/g, and all samples (except control samples) were diluted for ICPMS measurements to a mass concentration varying between 0.05 ng/g and 0.5 ng/g. The expanded uncertainties associated with the calculation of the gold mass concentration by ICPMS and sp-ICPMS were obtained according to the law of propagation of the variances of the related parameters following the "Guide to the Expression of Uncertainty in Measurement" [28].

2.4.2. Particle Size

The sizes of the gold nanoparticles are expressed as equivalent spherical diameters (ESDs) and were calculated based on the particle median intensity measured for the gold standard materials with known sizes (NIST RM8012 and BBI 60 nm). The equivalent spherical diameter was deduced from the standard particle diameter (Equation (1)). This calculation required a threshold to be set to distinguish nanoparticle intensity from background intensity:

$$d_p = \left(\frac{I_P - I_0}{R} \right)^{1/3} \quad (1)$$

where I_p is the intensity of a nanoparticle (cps), I_0 is the average intensity of the background (cps), and R is the slope of the linear regression between intensities and the cubed diameter of nanoparticles from the standard materials (cps/nm^3).

2.4.3. Particle Mass Concentration

Particle mass concentration represents the gold masses in suspension attributed to particles. According to IUPAC [29], since all dilutions were performed gravimetrically, it should be named particle mass fraction and be expressed for example in ng/g. However, to avoid confusion and to be

consistent with the particle number concentration (C_p, expressed as part/kg), the expression "particle mass concentration" is used throughout the text.

Particle mass concentration (C_m) was calculated by summing all intensities attributed to particles using a linear regression between intensities and elemental gold concentration (2):

$$C_m = \frac{t_{dwell} \cdot \sum (I_P - I_0)}{60 \cdot t_s \cdot K} \quad (2)$$

where C_m is the particle mass concentration (ng/g), t_{dwell} is the dwell time (ms), t_s is the total duration of a measurement (min), and K is the slope of the linear regression between intensities and elemental gold concentrations (cps/ng/g).

2.4.4. Number Particle Concentration and Transport Efficiency

The number particle concentration was calculated by counting the events attributed to nanoparticles during one measurement, considering the loss of sample in the spray chamber. Therefore, nebulization or transport efficiency needed to be estimated. Three different methods currently exist to estimate it: the frequency method, the size method, and the waste method [23]. In this study, we chose to use the size method, as it is easier to implement than the waste method and is based on the size of gold nanoparticle standard material rather than on the particle number concentration, for which no standard materials are currently available. The transport efficiency was determined by measuring three times two standards with different sizes (NIST RM8012 and BBI 60 nm). The relationship between intensities (cps) and cubed diameter was linear, with a correlation factor of 0.99998. The transport efficiency was 0.0595 ± 0.0020 (k = 1), which means that only about 6% of the gold from the samples reached the ICPMS plasma. Though not used in this study, the transport efficiency was also determined in the same measurements session as the frequency method and had a similar value at 0.0602 ± 0.0085 (k = 1).

The number particle concentration (C_p) was then determined according to Equation (3):

$$C_p = \frac{N_p}{Q \cdot \eta_{size} \cdot t_s} \cdot 10^3 \quad (3)$$

where C_p is the particle number concentration (part/kg), N_p is the number of detected nanoparticles, Q is the sample uptake rate (g/min), and η_{size} is the transport efficiency.

3. Results and Discussion

3.1. Optimization of Sp-ICPMS Measurements

Measurements by sp-ICPMS with time scans (or dwell time) between 1 ms and 10 ms are based on the hypothesis that only one nanoparticle is detected during each scan. If the dwell time is too long or too short, unwanted events such as double particle events (i.e., two particles detected during the same time scan), or partial events (i.e., the same particle counted twice in two consecutive time scans) may occur. To achieve the best measurement conditions, both dwell time and particle concentrations should be optimized. Laborda et al. [30] estimated that with a 5 ms dwell time and a particle flux reaching plasma comprised of between 4.7 NP/s and 15.2 NP/s, the probability of double events is between 0.03% and 0.28%, which corresponds to 1.3% and 3.8% of the total particle count, respectively. Following these results, we conducted our experiments in order to keep the particle fluxes below 15.2 NP/s. Figure 2 shows the results of the analysis of NIST RM8012 30 nm gold nanoparticles with varying dwell times. Concentrations and analysis duration were adapted in order to approximately obtain 3000 particle events for each tested dwell time. Since the duration of nanoparticle event detection in ICPMS is ca. 300–400 µs [31], a 1 ms dwell time should be sufficient for the measurement of one single nanoparticle. But such short dwell times tend to increase the amount of nanoparticle partial detection. In fact, it has been shown that a 5 ms dwell time results in less than 10% partial detection,

whereas this ratio could reach almost 30% for a 1 ms dwell time [32]. This is illustrated in Figure 2a, where, with a 1 ms dwell time, the nanoparticle peak was not clearly visible from the background. With 5 ms of dwell time (Figure 2b), the nanoparticle peak was best separated. Although none of these histograms shows perfect distinction between background and particles, we performed our analysis with 5 ms, which we considered to be the best condition.

The determination of the threshold between particles and background is crucial for sp-ICPMS measurements. Various published methods exist to determine this limit or cut-off, such as using the standard deviation of the background or the n-sigma iterative method [33]. However, as previously observed for AuNP measurements on the same instrument, these methods could not be applied in our case, as they result in limits that are either too low or too high [17]. As a consequence, we calculated the average 99.9 centile intensity of all blank measurements of 1% TMAH and used this intensity value as the limit ($I_{cut\text{-}off}$) between background and particles. Using the 99.9 centile meant that an average of 7 particles/min were detected in the 1% TMAH blank. This method resulted in a limit that was visually consistent and gave excellent results for all experiments in terms of both gold yields and size (Figure 3).

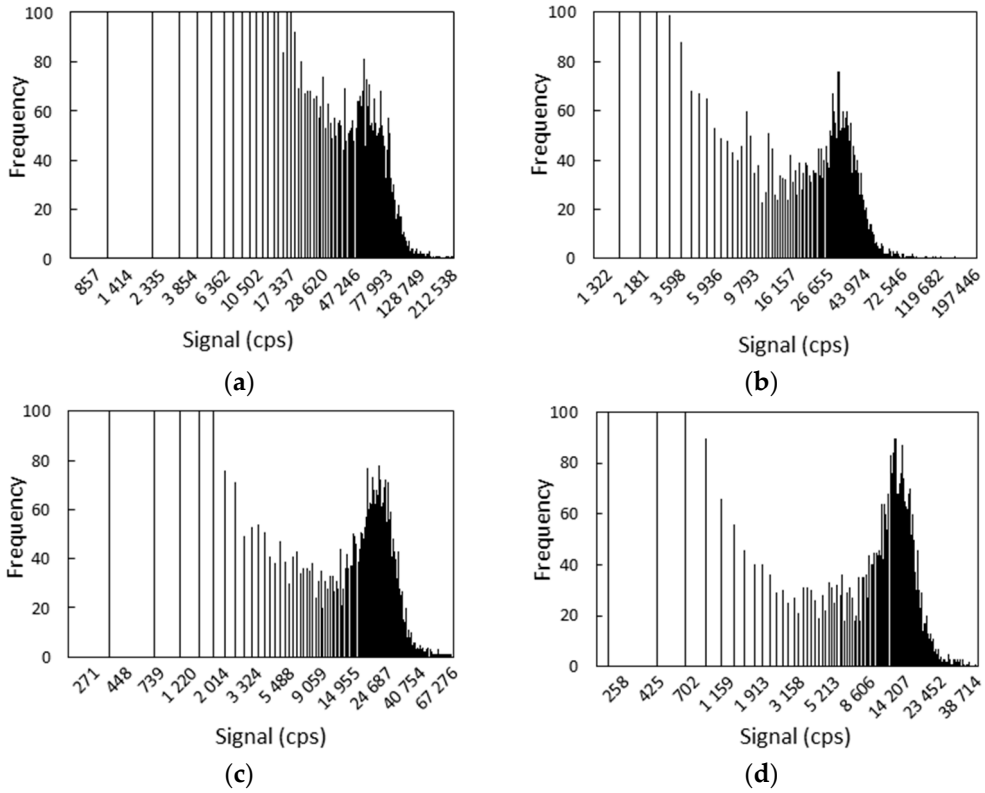

Figure 2. Histograms of signals obtained for a NIST RM8012 suspension with the following dwell time, analysis time, and gold concentrations: (**a**) 1 ms, 1 min, and 23.2 ng/kg; (**b**) 2 ms, 2 min, and 9.8 ng/kg; (**c**) 3 ms, 3 min, and 8.0 ng/kg; (**d**) 5 ms, 5 min, and 4.9 ng/kg. Note that the *x* axis has nonlinear scale to better display the limit between background and particles.

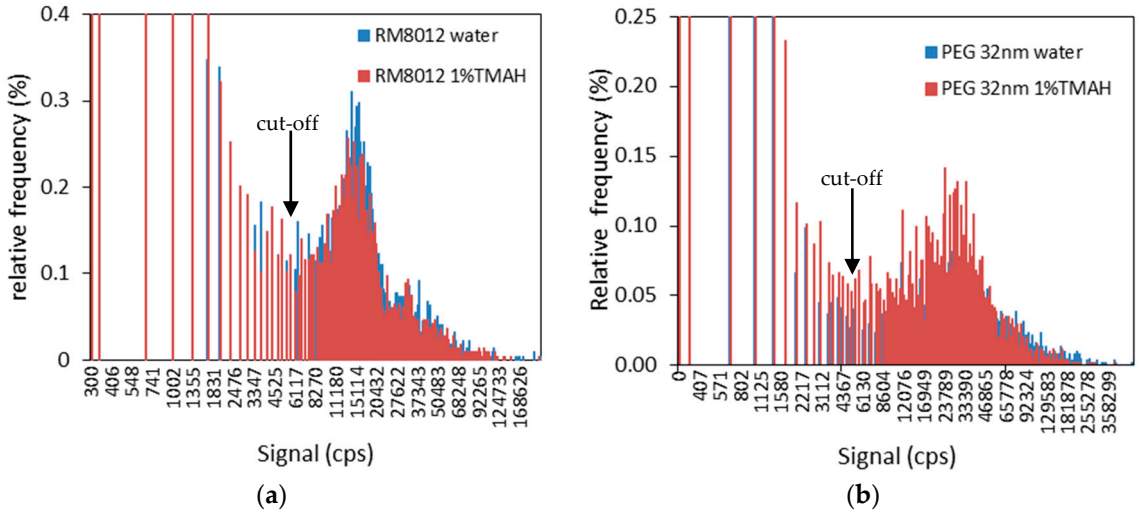

Figure 3. Histogram of signals obtained with a 5 ms dwell time in ultrapure water and 1% TMAH matrix for (**a**) NIST RM8012 and (**b**) PEGylated 32 nm gold nanoparticles suspensions.

3.2. Effect of Sample Preparation

Matrix effects can occur in ICPMS due to the presence of large amounts of matrix ions, resulting in plasma destabilization and loss of ions from the plasma to the detector. These matrix effects are usually considered negligible in highly diluted solutions, but TMAH and the ions coming from the dissolved solids and solubilized molecules originating from the cells may still affect nanoparticle ionization and transfer. In addition, digestion and dilution in TMAH may destabilize the gold nanoparticles.

We first checked that the same results were obtained in terms of size and peak shape in ultrapure water and in 1% TMAH. According to Figure 3, the signal distributions and the peak shapes were similar in both matrices, showing no effect of the dilution in 1% TMAH, neither on NIST RM8012 particles nor on the 32 nm PEGylated AuNPs used in the present study.

Then the effect of the digestion on particles in water and on control cells spiked with particles was studied. Higher TMAH concentrations (20%) were used by Gray et al. [20] to extract gold and silver particles with good results, but led in our case to a complete loss of particles for both nanoparticle types after one night (not shown here). Whether this loss occurred by dissolution or aggregation is unclear at this stage. Indeed, a loss by dissolution would have resulted in a signal too low to be distinguished from the blank after dilution, and a loss by aggregation could have resulted in the simple loss of particles by sedimentation in the vial. It was therefore found necessary to keep TMAH concentration low (5%) and to add BSA to preserve the particles, as proposed by Loeschner et al. [17]. The different results obtained with 20% TMAH on apparently similar biological samples may have come from the nature of the nanoparticles. Although they were both AuNPs, the ones from Gray et al. were much larger (100 nm) and had a polyvinylpyrrolidone (PVP) coating, whereas our nanoparticles were smaller and either citrate-stabilized or PEGylated. Further investigations would be required to really understand the effect of TMAH on these various particles and their coatings.

3.3. Gold Recovery and Size Measurements

In order to compare the gold masses obtained by acid digestion followed by ICPMS to those obtained by alkaline digestion followed by sp-ICPMS measurements, the E_N numbers were calculated according to ISO/IEC 17043 [34] using the uncertainty associated with each sample and each technique (Table 3). The aim of the E_N number is to estimate a deviation from a reference value, here the ICPMS bulk gold measurements.

Table 3. Sp-ICPMS and ICPMS analysis of the tumor cell samples: d_{50} and d_{avg} are the median and average diameters, respectively; C_m is gold mass per pellet; SD is the standard deviation; U is the expanded uncertainty on the gold masses; C_p is the particle number per pellet. E_N numbers were calculated for the gold masses between the ICPMS and the sp-ICPMS measurements of the same samples. N is the number of independent dilutions analyzed.

	sp-ICPMS								ICPMS				
Cell Samples	d_{50} **nm**	d_{avg} **nm**	C_p 10^7 **Part**	**SD**	C_m **µg**	**SD**	U (k = 2)	N	C_m **µg**	**SD**	U (k = 2)	N	E_N
MDAMB231 (control)	-	-	-	-	<0.009	-	-	1	<0.006	-	-	1	-
MDAMB231 (6 h)	32	32	4.8	-	0.019	-	0.003	1	0.020	0.001	0.004	2	0.3
MDAMB231 (24 h)	33	33	41.5	11.8	0.152	0.009	0.031	2	0.123	0.001	0.007	2	0.9
T47D (control)	-	-	-	-	<0.004	-	-	1	<0.006	-	-	1	-
T47D (6 h)	32	32	3.3	0.4	0.014	0.001	0.003	2	0.015	0.001	0.003	2	0.2
T47D (24 h)	32	32	14.9	5	0.057	0.014	0.029	2	0.067	0.007	0.013	2	0.3
T47D (test)	31	31	56	-	0.194	-	0.041	1	0.223	-	0.037	1	0.6

All E_N numbers were below 1, which indicated that the gold masses measured by sp-ICPMS were not significantly different from the ones estimated with ICPMS. The total gold yields were 97% on average for the cell samples. This validated our alkaline procedure for gold nanoparticle extraction from cells and confirmed that alkaline extraction resulted in total gold recovery.

The limit of detection in size was calculated using the cut-off intensity to determine the minimum measurable diameter, which was 18 nm. This value was in agreement with previously published limits of detection in size with quadrupole sp-ICPMS [35]. The median diameter of the PEG AuNPs was 31 nm, and the average diameter was 32 nm, in total agreement with the TEM measurements on these nanoparticles (Figure 1). For the cell samples, the median and the average diameters were similar, and ranged from 31 nm to 33 nm (Table 4). The shapes of the size distributions are shown on Figure 4. They were not different from the initial gold suspension (Figure 4f).

Table 4. Comparison of the average number of nanoparticles per cell between the three methods of quantification: particle number counting with sp-ICPMS (a), particle mass with sp-ICPMS (b), and particle mass with ICPMS (c). RSD: Relative Standard Deviation.

Cell Samples	Part/Cell (a)	Part/Cell (b)	Part/Cell (c)	Mean	RSD
MDAMB231 (6 h)	24	28	30	27	11%
MDAMB231 (24 h)	184	190	154	176	11%
T47D (6 h)	13	17	18	16	15%
T47D (24 h)	67	77	90	78	15%

Thus sp-ICPMS indicated that the gold nanoparticles were not modified in size upon tumor cell uptake in any of the tested cells after 6 and 24 h of exposure. In primary human endothelial cells, no size modification upon uptake was observed by sp-ICPMS upon gold nanoparticle uptake [14]. Indeed, gold nanoparticles are highly resistant and can be used to encapsulate more fragile particles [36]. No aggregation of the nanoparticles was observed in our analysis. It cannot, however, be excluded that the sample preparation with TMAH may have separated particles that were agglomerated in the cells.

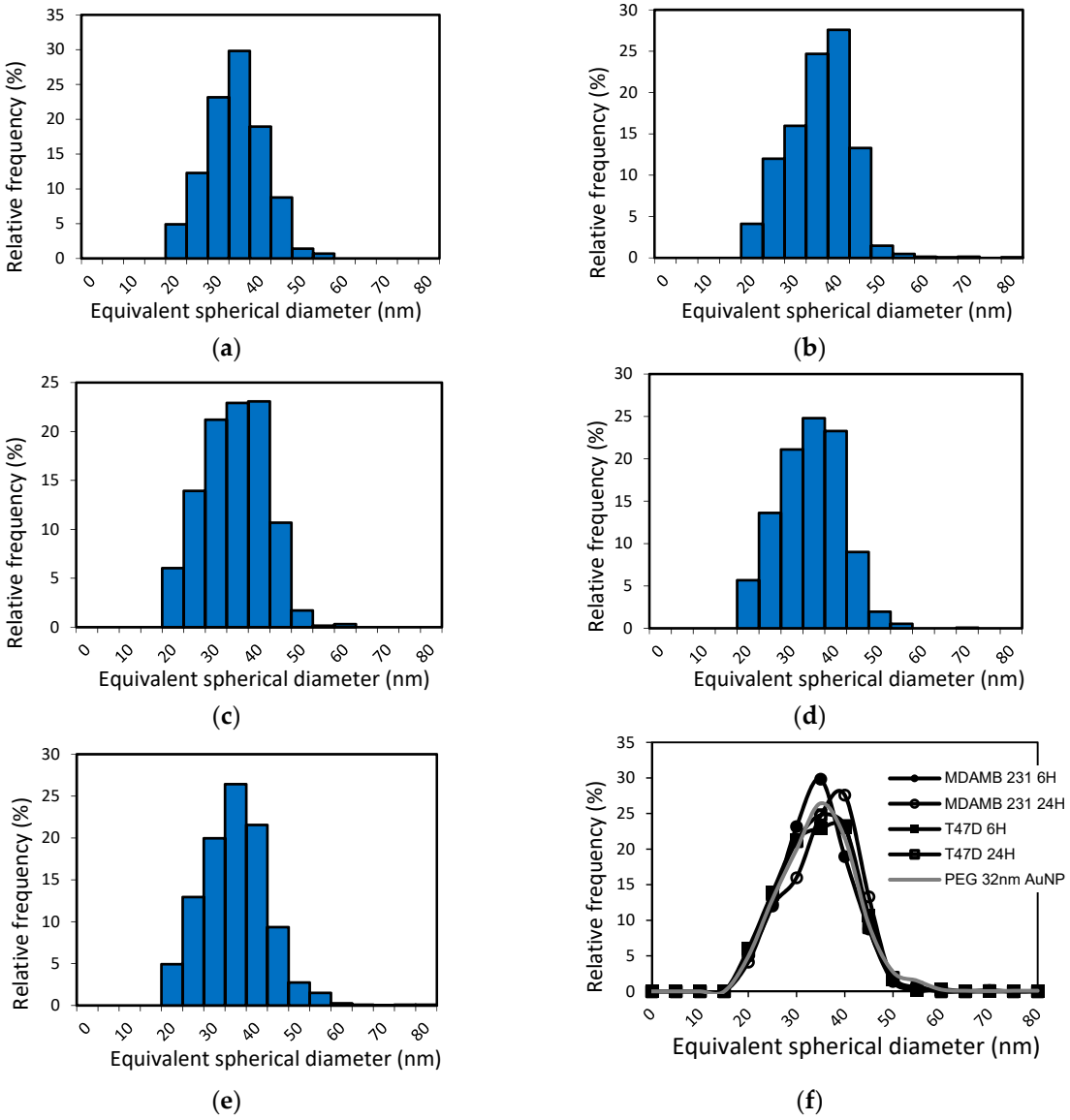

Figure 4. Size distribution of gold nanoparticles in the tumor cells and in suspension: (**a**) MDAMB231 (6 h); (**b**) MDAMB 231 (24 h); (**c**) T47D (6 h); (**d**) T47D (24 h); (**e**) 32 nm PEGylated AuNPs; (**f**) all together.

3.4. Average Particle Number Per Cell

For comparison to the sp-ICPMS results, the particle number concentration could be estimated with a second method, knowing the particle mass concentration and the average particle diameter:

$$C_p = \frac{C_m}{\frac{4}{3}\pi\rho_{Au}\left(\frac{d}{2}\right)^3} \cdot 10^9 \quad (4)$$

where C_p is the particle number concentration (part/kg) and C_m is the particle mass concentration (ng/g).

We thus compared the average particle number per cell calculated by three methods. The first method, (a), was the sp-ICPMS particle counting based on Equation (3). The second method, (b), was based on the sp-ICPMS total gold mass per pellet and d_{avg} of the particles (Equation (4)). The third one, (c), was based on ICPMS gold mass and d_{avg} of the particles (Equation (4)).

As shown in Table 4, these three methods displayed very similar results with a good relative standard deviation (RSD) between 11% and 15%. It demonstrated that the particle number determined

by counting the particles by sp-ICPMS was consistent with the gold masses obtained. Since no reference material for particle numbers currently exists, this is a first approach in validating particle number measurements.

The mean values for the number of particles per cell ranged from 16 to 176 depending on the cell line and duration of exposure. Overall, the uptake of gold nanoparticles into MDAMB231 cells was twice as high as into T47D cells, whatever the time of exposure, illustrating how important the quantification of nanoparticle uptake within the cells is for understanding AuNP biological effects. Such differences between cell lines have been reported in several publications but have not been rationalized yet [37–39]. For comparison, in MDAMB231 cells incubated with 14 or 50 nm AuNPs functionalized by thiolated PEG of MW 2000, Cruje and Chithrani found 160 or 40 particles per cell, respectively, which is consistent with our results [37].

4. Conclusions

Our work showed that analysis by sp-ICPMS is a suitable tool in studying the uptake of particles at the cellular level. This is relevant for nanomedical applications, but also for nanotoxicological studies where the internalized concentration is of interest. It allows retrieving the size distribution and the average concentration of particles in a cell sample, which is not possible by classical ICPMS analysis. Calculation of particle number per cell based on ICPMS gold mass and average particle diameter might be possible in the case of monomodal AuNPs (as in this study), but is not possible if (a) the particle size is unknown, (b) the particles have a broad size distribution, and (c) the material is not only present in the form of NPs. In these cases, sp-ICPMS can be a suitable technique. TEM analysis is not quantitative regarding NP number per cell, but can provide additional information about NP localization, agglomeration and aggregation (typically not distinguishable) in the cells. Care must still be taken when applying a digestion method for sp-ICPMS, as several methods currently exist, but they cannot be applied to all samples and nanoparticles. In addition, the effects of sample preparation on the particles are not well understood and prevent definitive conclusions on the likelihood of aggregation upon cell uptake. More work is needed to understand these differences and to be able in the future to propose more versatile and controlled sample preparation methods.

Author Contributions: J.N., R.G., K.L., P.F., and S.C. conceived and designed the experiments; J.N., R.G., M.H., C.S.-R., E.B. and C.O. performed the experiments; J.N. wrote the paper; all authors contributed to editing the paper.

Funding: This work was funded by the French metrology 2018 program and benefited from the DRF Impulsion (CEA) and CYTOMETRY/ELECTRONIC MICROSCOPY/LIGHT MICROSCOPY facility of Imagerie-Gif, (http://www.i2bc.paris-saclay.fr), a member of IBiSA (http://www.ibisa.net), supported by "France-BioImaging" (ANR-10-INBS-04-01), and the Labex "Saclay Plant Science" (ANR-11-IDEX-0003-02).

Acknowledgments: Jialan Wang, Enrica Alasonati, and Daniela Stoica are deeply thanked for their help and discussions on this project.

Conflicts of Interest: The authors declare no conflicts of interest. The founding sponsors had no role in the design of the study; in the collection, analyses, or interpretation of data; in the writing of the manuscript; or in the decision to publish the results.

References

1. Bobo, D.; Robinson, K.J.; Islam, J.; Thurecht, K.J.; Corrie, S.R. Nanoparticle-Based Medicines: A Review of FDA-Approved Materials and Clinical Trials to Date. *Pharm. Res.* **2016**, *33*, 2373–2387. [CrossRef] [PubMed]
2. Jain, S.; Hirst, D.G.; O'Sullivan, J.M. Gold nanoparticles as novel agents for cancer therapy. *Br. J. Radiol.* **2012**, *85*, 101–113. [CrossRef] [PubMed]
3. Hadioui, M.; Merdzan, V.; Wilkinson, K.J. Detection and Characterization of ZnO Nanoparticles in Surface and Waste Waters Using Single Particle ICPMS. *Environ. Sci. Technol.* **2015**, *49*, 6141–6148. [CrossRef] [PubMed]
4. Adeleye, A.S.; Pokhrel, S.; Mädler, L.; Keller, A.A. Influence of nanoparticle doping on the colloidal stability and toxicity of copper oxide nanoparticles in synthetic and natural waters. *Water Res.* **2018**, *132*, 12–22. [CrossRef] [PubMed]

5. Peters, R.J.B.; van Bemmel, G.; Herrera-Rivera, Z.; Helsper, H.P.F.G.; Marvin, H.J.P.; Weigel, S.; Tromp, P.C.; Oomen, A.G.; Rietveld, A.G.; Bouwmeester, H. Characterization of titanium dioxide nanoparticles in food products: Analytical methods to define nanoparticles. *Agric. Food Chem.* **2014**, *62*, 6285–6293. [CrossRef] [PubMed]
6. Loeschner, K.; Correia, M.; Chaves, C.L.; Rokkjær, I.; Sloth, J.J. Detection and characterization of aluminium-containing nanoparticles in Chinese noodles by single particle ICP-MS. *Food Addit. Contam. Part A* **2018**, *35*, 86–93. [CrossRef] [PubMed]
7. Dan, Y.; Shi, H.; Stephan, C.; Liang, X. Rapid analysis of titanium dioxide nanoparticles in sunscreens using single particle inductively coupled plasma-mass spectrometry. *Microchem. J.* **2015**, *122*, 119–126. [CrossRef]
8. de la Calle, I.; Menta, M.; Klein, M.; Séby, F. Screening of TiO_2 and Au nanoparticles in cosmetics and determination of elemental impurities by multiple techniques (DLS, SP-ICP-MS, ICP-MS and ICP-OES). *Talanta* **2017**, *171*, 291–306. [CrossRef]
9. Adeleye, A.S.; Oranu, E.A.; Tao, M.; Keller, A.A. Release and detection of nanosized copper from a commercial antifouling paint. *Water Res.* **2016**, *102*, 374–382. [CrossRef]
10. Bao, D.; Oh, Z.G.; Chen, Z. Characterization of Silver Nanoparticles Internalized by Arabidopsis Plants Using Single Particle ICP-MS Analysis. *Plant Sci.* **2016**, *7*, 32. [CrossRef]
11. Dan, Y.; Zhang, W.; Xue, R.; Ma, X.; Stephan, C.; Shi, H. Characterization of gold nanoparticle uptake by tomato plants using enzymatic extraction followed by single-particle Inductively Coupled plasma-mass spectrometry analysis. *Environ. Sci. Technol.* **2015**, *49*, 3007–3014. [CrossRef] [PubMed]
12. Jimenez-Lamana, J.; Wojcieszek, J.; Jakubiak, M.; Asztemborska, M.; Szpunar, J. Single particle ICP-MS characterization of platinum nanoparticles uptake and bioaccumulation by *Lepidium sativum* and *Sinapis alba* plants. *J. Anal. Atomic Spectrom.* **2016**, *31*, 2321–2329. [CrossRef]
13. Keller, A.A.; Huang, Y.; Nelson, J. Detection of nanoparticles in edible plant tissues exposed to nano-copper using single-particle ICP-MS. *J. Nanopart. Res.* **2018**, *20*, 101. [CrossRef]
14. Klingberg, H.; Oddershede, L.B.; Loeschner, K.; Larsen, E.H.; Loft, S.; Møller, P. Uptake of gold nanoparticles in primary human endothelial cells. *Toxicol. Res.* **2015**, *4*, 655–666. [CrossRef]
15. Kińska, K.; Jiménez-Lamana, J.; Kowalska, J.; Krasnodębska-Ostręga, B.; Szpunar, J. Study of the uptake and bioaccumulation of palladium nanoparticles by Sinapis alba using single particle ICP-MS. *Sci. Total Environ.* **2018**, *615*, 1078–1085. [CrossRef] [PubMed]
16. Dan, Y.; Ma, X.; Zhang, W.; Liu, K.; Stephan, C.; Shi, H. Single particle ICP-MS method development for the determination of plant uptake and accumulation of CeO_2 nanoparticles. *Anal. Bioanal. Chem.* **2016**, *408*, 5157–5167. [CrossRef] [PubMed]
17. Loeschner, K.; Brabrand, M.S.J.; Sloth, J.J.; Larsen, E.H. Use of alkaline or enzymatic sample pretreatment prior to characterization of gold nanoparticles in animal tissue by single-particle ICPMS. *Anal. Bioanal. Chem.* **2014**, *406*, 3845–3851. [CrossRef] [PubMed]
18. Vidmar, J.; Buerki-Thurnherr, T.; Loeschner, K. Comparison of the suitability of alkaline or enzymatic sample pre-treatment for characterization of silver nanoparticles in human tissue by single particle ICP-MS. *J. Anal. Atomic Spectrom.* **2018**, *33*, 752–761. [CrossRef]
19. Peters, R.J.B.; Rivera, Z.H.; van Bemmel, G.; Marvin, H.J.P.; Weigel, S.; Bouwmeester, H. Development and validation of single particle ICP-MS for sizing and quantitative determination of nano-silver in chicken meat. *Anal. Bioanal. Chem.* **2014**, *406*, 3875–3885. [CrossRef]
20. Gray, E.P.; Coleman, J.; Bednar, A.; Kennedy, A.J.; Ranville, J.F.; Higgins, C.P. Extraction and analysis of silver and gold nanoparticles from biological tissues using single particle inductively coupled plasma mass spectrometry. *Environ. Sci. Technol.* **2013**, *47*, 14315–14323. [CrossRef]
21. Jokerst, J.V.; Lobovkina, T.; Zare, R.N.; Gambhir, S.S. Nanoparticle PEGylation for imaging and therapy. *Nanomedicine* **2011**, *6*, 715–728. [CrossRef] [PubMed]
22. Peters, R.; Herrera-Rivera, Z.; Undas, A.; van der Lee, M.; Marvin, H.; Bouwmeester, H.; Weigel, S. Single particle ICP-MS combined with a data evaluation tool as a routine technique for the analysis of nanoparticles in complex matrices. *J. Anal. Atomic Spectrom.* **2015**, *30*, 1274–1285. [CrossRef]
23. Pace, H.E.; Rogers, N.J.; Jarolimek, C.; Coleman, V.A.; Higgins, C.P.; Ranville, J.F. Determining Transport Efficiency for the Purpose of Counting and Sizing Nanoparticles via Single Particle Inductively Coupled Plasma Mass Spectrometry. *Anal. Chem.* **2011**, *83*, 9361–9369. [CrossRef] [PubMed]
24. Turkevich, J. Colloidal gold. Part I. *Gold Bull.* **1985**, *18*, 86–91. [CrossRef]

25. Gilles, M.; Brun, E.; Sicard-Roselli, C. Gold nanoparticles functionalization notably decreases radiosensitization through hydroxyl radical production under ionizing radiation. *Colloids Surf. B Biointerfaces* **2014**, *123*, 770–777. [CrossRef] [PubMed]
26. Xia, X.; Yang, M.; Wang, Y.; Zheng, Y.; Li, Q.; Chen, J.; Xia, Y. Quantifying the Coverage Density of Poly(ethylene glycol) Chains on the Surface of Gold Nanostructures. *ACS Nano* **2012**, *6*, 512–522. [CrossRef] [PubMed]
27. International Organization for Standardization. *Nanotechnologies—Size Distribution and Concentration of Inorganic Nanoparticles in Aqueous Media via Single Particle Inductively Coupled Plasma Mass Spectrometry*; XP ISO/TS 19590:20178; International Organization for Standardization: Geneva, Switzerland, 2017.
28. Joint Committee for Guides in Metrology. *Evaluation of Measurement Data—Guide to the Expression of Uncertainty in Measurement*; JCGM 100:2008; Joint Committee for Guides in Metrology: Paris, France, 2008.
29. Cohen, E.R.; Cvitas, T.; Frey, J.G.; Holmström, B.; Kuchitsu, K.; Marquardt, R.; Mills, I.; Pavese, F.; Quack, M.; Stohner, J.; et al. *Quantities, Units and Symbols in Physical Chemistry*, 3rd ed.; IUPAC Green Book; IUPAC & RSC Publishing: Cambridge, UK, 2008.
30. Laborda, F.; Jiménez-Lamana, J.; Bolea, E.; Castillo, J.R. Critical considerations for the determination of nanoparticle number concentrations, size and number size distributions by single particle ICP-MS. *J. Anal. Atomic Spectrom.* **2013**, *28*, 1220–1232. [CrossRef]
31. Hineman, A.; Stephan, C. Effect of dwell time on single particle inductively coupled plasma mass spectrometry data acquisition quality. *J. Anal. Atomic Spectrom.* **2014**, *29*, 1252–1257. [CrossRef]
32. Liu, J.; Murphy, K.E.; MacCuspie, R.I.; Winchester, M.R. Capabilities of Single Particle Inductively Coupled Plasma Mass Spectrometry for the Size Measurement of Nanoparticles: A Case Study on Gold Nanoparticles. *Anal. Chem.* **2014**, *86*, 3405–3414. [CrossRef] [PubMed]
33. Tuoriniemi, J.; Cornelis, G.; Hassellöv, M. Size discrimination and detection capabilities of single-particle ICP-MS for environmental analysis of silver nanoparticles. *Anal. Chem.* **2012**, *29*, 743–752. [CrossRef]
34. International Organization for Standardization. *Conformity Assessment—General Requirements for Proficiency Testing*; NF EN ISO/CEI 17043:2010; International Organization for Standardization: Geneva, Switzerland, 2010.
35. Lee, S.; Bi, X.; Reed, R.B.; Ranville, J.F.; Herckes, P.; Westerhoff, P. Nanoparticle Size Detection Limits by Single Particle ICP-MS for 40 Elements. *Environ. Sci. Technol.* **2014**, *48*, 10291–10300. [CrossRef] [PubMed]
36. Espinosa, A.; Curcio, A.; Cabana, S.; Radtke, G.; Bugnet, M.; Kolosnjaj-Tabi, J.; Péchoux, C.; Alvarez-Lorenzo, C.; Botton, G.A.; Silva, A.K.A.; et al. Intracellular Biodegradation of Ag Nanoparticles, Storage in Ferritin, and Protection by a Au Shell for Enhanced Photothermal Therapy. *ACS Nano* **2018**. [CrossRef] [PubMed]
37. Cruje, C.; Chithrani, B.D. Integration of Peptides for Enhanced Uptake of PEGylated Gold Nanoparticles. *J. Nanosci. Nanotechnol.* **2015**, *15*, 2125–2131. [CrossRef] [PubMed]
38. Unciti-Broceta, J.D.; Cano-Cortés, V.; Altea-Manzano, P.; Pernagallo, S.; Díaz-Mochón, J.J.; Sánchez-Martín, R.M. Number of Nanoparticles per Cell through a Spectrophotometric Method—A key parameter to Assess Nanoparticle-based Cellular Assays. *Sci. Rep.* **2015**, *5*, 10091. [CrossRef] [PubMed]
39. Coulter, J.A.; Jain, S.; Butterworth, K.T.; Taggart, L.E.; Dickson, G.R.; McMahon, S.J.; Hyland, W.B.; Muir, M.F.; Trainor, C.; Hounsell, A.R.; et al. Cell type-dependent uptake, localization, and cytotoxicity of 1.9 nm gold nanoparticles. *Int. J. Nanomed.* **2012**, *7*, 2673–2685. [CrossRef] [PubMed]